Crystallographic and Molecular Orbital Studies of 4-Oxopyrazole 1,2-Dioxides. An Exceptionally Elongated N–N Bond

Yasuyuki Yoshitake, Masashi Eto, and Kazunobu Harano*

Faculty of Pharmaceutical Sciences, Kumamoto University, 5–1 Oe-honmachi, Kumamoto 862–0973, Japan.

Received September 28, 1998; accepted January 26, 1999

An X-ray analysis of 3,5-dimethyl-4-oxopyrazole 1,2-dioxide (1) reveals that the N–N bond is considerably elongated [1.659(5) Å]. The bond length calculated by *ab initio* significantly varied with the change of the calculation level. The bond elongation is considered to arise from the dipole–dipole repulsion between the $>N \rightarrow O$ groups enhanced by the antiaromatic character of the unique ring system.

Key words 4-oxopyrazole 1,2-dioxide; single crystal X-ray analysis; *ab initio*; AM1; bond elongation; aromaticity

During our studies[1)] on the 1,3-dipolar cycloaddition behavior of 3,5-disubstituted 4-oxopyrazole 1,2-dioxides toward various unsaturated compounds, we found that the 1,3-dipoles showed enhanced *endo* selectivity toward dipolarophiles having an ether or a carbonyl functional group and the PM3 structure optimization of 4-oxopyrazole 1,2-dioxide predicted a remarkably long N–N bond (1.742 Å). In connection with this, we recently communicated the role of the orientation complex (OC) between 4-oxopyrazole 1,2-dioxide and the dipolarophiles before formation of the transition state (TS).[1d)]

The unusual structural features of 3,5-dimethyl-4-oxopyrazole 1,2-dioxide (**1**) are discussed here in detail based on its refined X-ray data and further additional data that we have obtained.

Results

Materials 3,5-Dimethyl-4-oxopyrazole 1,2-dioxide was prepared by the reported method.[2)]

X-Ray Crystallography Crystal data; $C_5H_6N_2O_3$ (**1**), M.W.=142.1. Orthorhombic, space group $P2_12_12_1$, $a=9.695(3)$, $b=14.986(2)$, $c=4.668(3)$ Å, $V=678.1(4)$ Å^3, $Dc=1.392$ gcm^{-3}, $Z=4$. Single crystals of dimethyl 4-oxopyrazole 1,2-dioxide (**1**) suitable for X-ray analysis were prepared by slow evaporation of an ethanol–acetone solution at room temperature. Crystals are bright yellow needles. Intensity data were collected on a Rigaku AFC7R four-circle automated diffractometer with a graphite monochromated Mo-K_α radiation (50 kV–150 mA), and rotating anode generator. A total of 933 reflections was collected. The intensities of three representative reflections were measured after every 150 reflections. Over the course of data collection, the standards decreased by 27.3%. A linear correction factor was applied to the data to account for this phenomenon. The structure was solved by the direct method (SIR92)[3)] and expanded using Fourier techniques (DIRDIF94).[4)] The non-hydrogen atoms were refined anisotropically with a full-matrix program (9.03%). At this stage, the three hydrogen atoms of one methyl group were located on a difference Fourier map and refined isotropically and the other methyl hydrogens were placed in calculated positions from the molecular symmetry and were included in fixed positions. The final cycle of full-matrix least-squares refinement was based on 656 observed reflections ($I>3.00\sigma(I)$) and 104 variable parameters and converged (largest parameter shift was 0.43 times its esd) with unweighted (R) and weighted agreement factors (Rw) of 0.052 and 0.042, respectively. All calculations were performed using the teXsan[5)] crystal structure analysis package on a Silicon Graphics IRIS Indigo work station (WS).

The final atomic coordinates and thermal parameters are shown in Table 1.

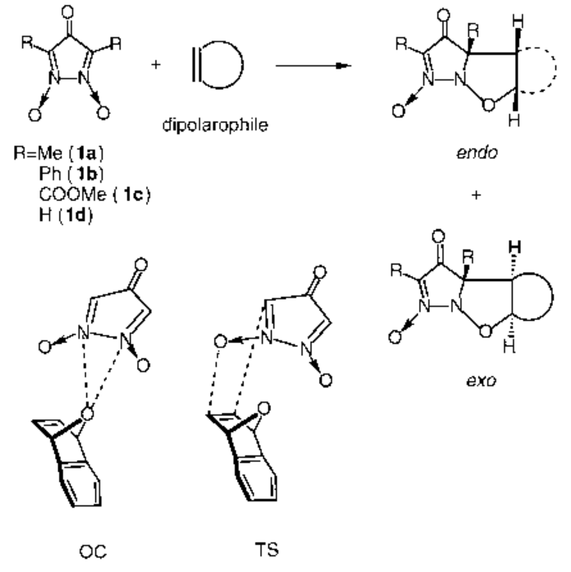

Chart 1

Table 1. Atomic Coordinates

Atom	*x*	*y*	*z*
O(6)	0.2080(2)	0.0644(1)	0.7668(4)
O(8)	0.0421(2)	0.2342(1)	0.0212(5)
O(9)	−0.1170(2)	0.0853(1)	0.0484(5)
N(3)	0.0734(2)	0.1808(1	0.2116(5)
N(4)	−0.0241(2)	0.0899(1)	0.2273(5)
C(1)	0.1422(2)	0.0894(2)	0.5662(5)
C(2)	0.1645(3)	0.1742(2)	0.4103(6)
C(5)	0.0248(2)	0.0425(2)	0.4357(6)
C(7)	0.2703(4)	0.2431(3	0.469(1)
C(10)	−0.0305(3)	−0.0449(2)	0.5168(9)
H(11)	0.279(4)	0.254(2)	0.655(9)
H(12)	0.347(3)	0.217(2)	0.371(9)
H(13)	0.250(3)	0.300(2)	0.406(9)
H(14)	0.0301	−0.092	0.4726
H(15	−0.0492	−0.0464	0.7211
H(16)	−0.1180	−0.0562	0.4226

---

* To whom correspondence should be addressed.

The ORTEP drawing and cell packing diagram of **1** are depicted in Figs.1 and 2, respectively. The bond distances are included in Fig. 1. The bond angles are listed in Table 2. Some intermolecular contacts are collected in Table 3.

MO Calculation Semi-empirical MO calculations were run through the ANCHOR II interface using MOPAC6.0[6] on a Fujitsu S4/2 WS or through the CS Chem3D Pro interface using MOPAC93 on a Macintosh 8500/150 personal computer. The *ab initio* computations,[7] were carried out on a Scientists' Paradise Dragon AXP5A/433 computer or a Convex Exemplar SPP-1000 parallel computer in the Kumamoto University Information Processing Center. The optimized structures calculated by AM1 or PM3 method was used as starting geometries for the *ab initio* calculations. Graphical analysis of the MO calculation data was performed on a Macintosh 8500/150 personal computer.

The structural data (bond lengths and angles) calculated by semiempirical and *ab initio* methods with various basis sets

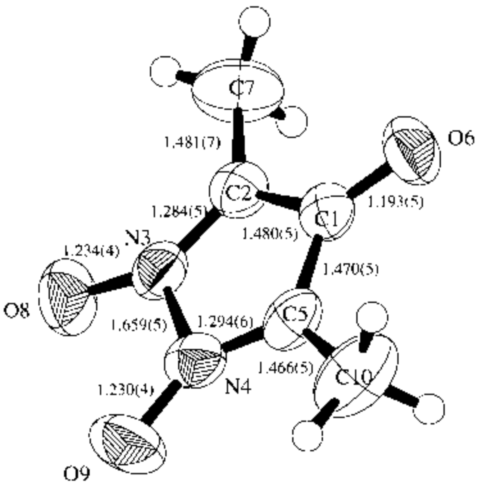

Fig. 1. ORTEP Drawing of **1**

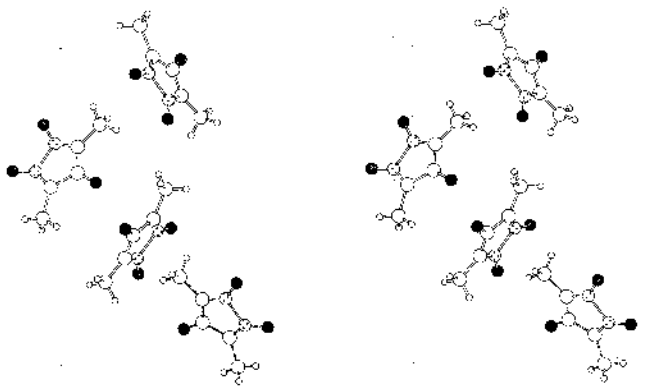

Fig. 2a. Stereoview of the Cell Packing Diagram of **1**

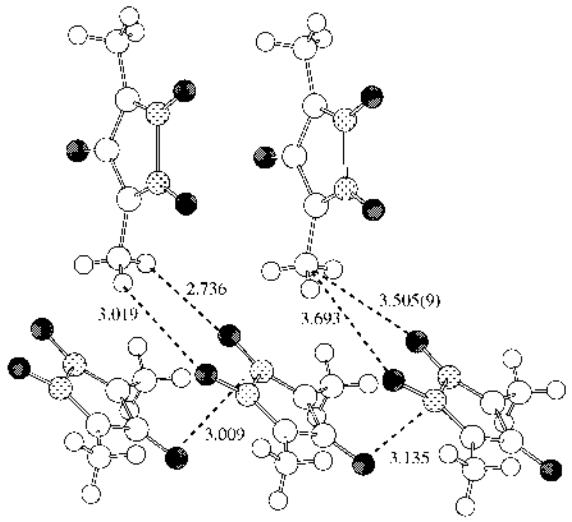

Fig. 2b. Intermolecular Interactions in Crystal of **1**

Table 2. Intramolecular Bond Angles

Atom	Angle (°)	Atom	Angle (°)
O(8)–N(3)–N(4)	115.1(3)	C(2)–C(1)–C(5)	108.6(4)
O(8)–N(3)–C(2)	137.6(4)	N(3)–C(2)–C(1)	108.7(4)
N(4)–N(3)–C(2)	107.3(3)	N(3)–C(2)–C(7)	123.8(5)
O(9)–N(4)–N(3)	115.7(4)	C(1)–C(2)–C(7)	127.5(5)
O(9)–N(4)–C(5)	138.3(4)	N(4)–C(5)–C(1)	109.4(4)
N(3)–N(4)–C(5)	106.0(3)	N(4)–C(5)–C(10)	123.4(5)
O(6)–C(1)–C(2)	125.2(4)	C(1)–C(5)–C(10)	127.1(5)
O(6)–C(1)–C(5)	126.1(4)		

Table 3. Intermolecular Distances Involving the Nonhydrogen Atoms

Atom	Atom	Distance (Å)	Symmetry[a] Operation	Atom	Atom	Distance (Å)	Symmetry[a] Operation
O(6)	N(3)	3.009(4)	I	O(8)	C(7)	3.400(9)	IV
O(6)	C(1)	3.062(5)	II	O(8)	C(7)	3.505(9)	VI
O(6)	N(4)	3.135(5)	I	O(8)	C(7)	3.567(9)	VII
O(6)	O(6)	3.137(4)	II	O(9)	C(5)	3.238(6)	IV
O(6)	O(6)	3.137(4)	III	O(9)	C(10)	3.266(7)	IV
O(6)	C(5)	3.146(5)	II	O(9)	C(1)	3.374(5)	IV
O(6)	O(8)	3.236(4)	I	O(9)	C(10)	3.473(6)	VIII
O(6)	C(10)	3.350(6)	II	O(9)	C(7)	3.590(8)	VII
O(6)	O(9)	3.429(4)	I	N(3)	C(1)	3.376(6)	IV
O(6)	C(2)	3.450(5)	I	N(3)	C(7)	3.487(8)	VII
O(8)	C(1)	3.188(5)	IV	N(4)	C(1)	3.482(5)	IV
O(8)	C(2)	3.217(6)	IV	N(4)	C(7)	3.500(7)	VII
O(8)	C(10)	3.316(6)	V				

a) The superscripts refer to the following equivalent positions: I: $x, y, 1+z$; II: $1/2-x, -y, 1/2+z$; III: $1/2-x, -y, -1/2+z$; IV: $x, y, 1-z$; V: $-x, 1/2+y, 1/2+z$; VI: $-1-x, 1/2+y, 1/2+z$; VII: $-1/2+x, 1/2-y, 1-z$; VIII: $-1/2-x, -y, -1/2+z$. Contacts within 3.60 angstroms. Estimated standard deviations in the least significant figure are given in parentheses.

Table 4. Bond Lengths (Å) and Angles (°) of **1d** Calculated by *Ab Initio* on the Different Levels

Method	N→O	N=C	N–N	C=O	C–C	C–N–O
X-ray	1.230(5)	1.284(5)	1.659(5)	1.193(5)	1.470(5)	137.6(4)
	1.234(4)	1.294(6)		1.481(5)	138.3(4)	
AM1	1.185	1.346	1.623	1.223	1.496	
PM3	1.209	1.328	1.730	1.205	1.496	
STO-3G	1.288	1.323	1.547	1.224	1.499	
3-21G	1.283	1.275	1.546	1.204	1.484	134.0
6-31G(d)[a]	1.208	1.277	1.518	1.186	1.482	
6-311G(d)[b]	1.199	1.277	1.524	1.181	1.481	
MP2/6-31G(d)[c]	1.213	1.317	1.806	1.238	1.470	141.2
B3LYP/6-31G(d)	1.214	1.300	1.723	1.220	1.482	
B3LYP/6-31G(d,p)	1.214	1.301	1.721	1.220	1.482	
B3LYP/6-311+G(d,p)	1.208	1.298	1.734	1.215	1.482	
B3LYP/6-311G(2d)	1.207	1.296	1.719	1.213	1.479	138.7
B3PW91/6-31G(2d)	1.204	1.298	1.683	1.213	1.476	
B3PW91/6-31+G(2d)	1.205	1.298	1.685	1.215	1.477	
B3PW91/6-31G(2df)	1.203	1.297	1.683	1.212	1.477	
B3PW91/6-31G(3df)	1.204	1.294	1.684	1.213	1.477	
B3PW91/6-311G(2d)	1.203	1.295	1.690	1.212	1.475	138.4

a) The same as 6-31G(d,p). *b*) The same as 6-311G(d,p). *c*) The same as MP2/6-31G(d,p).

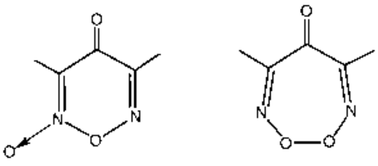
2 **3**

Fig. 3. Previously Proposed Structures of **1**

are summarized in Table 4.

Discussion

We tried to clarify the crystal structure of the 3,5-bis-(methoxycarbonyl), 3-methyl-5-phenyl or 3,5-diphenyl derivative of 4-oxopyrazole 1,2-dioxide. However, we could not obtain the corresponding single crystals suitable for X-ray analysis except for the 3,5-dimethyl derivative (**1**). As a result, only the analysis of **1** was successful. Figure 1 shows the crystal structure of **1**, ruling out the previously proposed structures (**2** and **3**).[2b] (Fig. 3)

As can be seen in Table 1, the N–N bond is exceptionally elongated [1.659(5) Å], indicating a fairly weak interaction. At first, we assumed that the N–N bond elongation arises from the intermolecular packing effects deduced from the presence of strong short contacts. The crystal packing diagram of **1** is depicted in Fig. 2. The molecules are arranged in a nearly parallel disposition (interplanar distance, *ca.* 3 Å) with a head-to-tail relationship, in which the two nitrogen atoms of **1** link with the carbonyl oxygen of an adjacent molecule and the linkage is reinforced by the hydrogen bondings between the methyl hydrogens and the oxygen atoms of the N–O groups.

The MO structure optimization (AM1) of the four molecules extracted from the crystal packing coordinates gave almost the same N–N bond length (Fig. 4), suggesting that the intermolecular donor–acceptor interaction in the crystal does not affect on the N–N bond elongation.

To find the origin of the bond elongation, we performed MO calculations on **1** and related compounds. The N–N bond length is significantly affected by the computational level, ranging from 1.518 to 1.806 Å. The HF/3-21G and 6-31G(d) values (1.546 and 1.518 Å) are remarkably shorter than the X-ray value [1.659(5) Å], whereas the MP2/6-31G(d) bond length (1.806 Å) is 0.147 Å longer than the observed value. The B3LYP/6-31G(d) bond length (1.723 Å) calculated with density functional theory (DFT) method is also 0.064 Å longer than the observed one. The B3LYP calculations with larger basis sets still overestimate the N–N bond length. The B3LYP/6-311G(2d) calculation gave 1.719 Å. In contrast, the B3PW91/6-31G(2d) and B3PW91/6-31G(2df) structures are close to experiment.

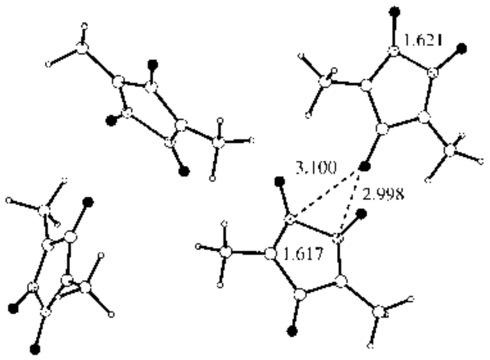

Fig. 4. AM1-Calculated Geometries of Intermolecular Interaction of **1**

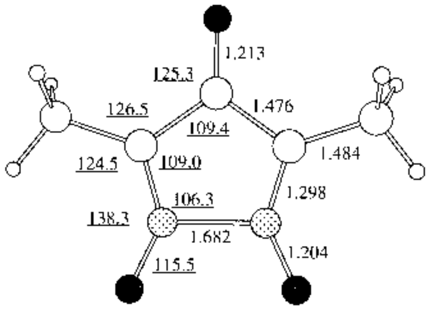

Fig. 5. B3PW91/6-31G(2d) Structure of **1**

Even in the B3PW91/6-31G(2d) geometry (Fig. 5), the N–N bond length (1.683 Å) is too long by 0.024 Å and the

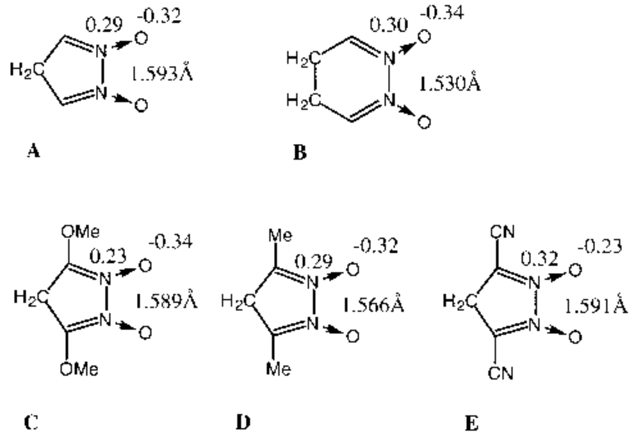

Fig. 6. AM1 N–N Bond Length of Some Model Compounds

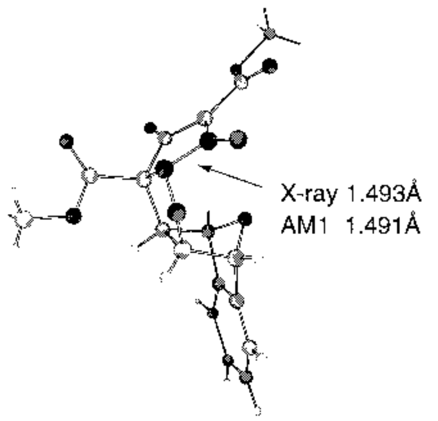

Fig. 7. X-Ray Structure of the Cycloadduct of 3,5-Bis(methoxycarbonyl)-4-oxopyrazole 1,2-Dioxide and Epoxynaphthalene

Table 5. The N–N Bond Lengths and Net Charges of Model Compounds Calculated by AM1 and *Ab Initio* at Different Levels of Theory

Method	Bond	F	G	H	I	J
AM1	**N–N**	**1.662 Å**	**1.600 Å**	**1.585 Å**	**1.577 Å**	**1.551 Å**
	NC_N	0.303	0.288	0.284	0.289	0.277
	NC_O	−0.254	−0.304	−0.316	−0.317	−0.346
	C=N	1.334 Å	1.342 Å	1.344 Å	1.346 Å	1.350 Å
	C–C	1.491 Å	1.475 Å	1.472 Å	1.468 Å	1.462 Å
RHF/3-21G	**N–N**	**1.569 Å**	**1.509 Å**	**1.484 Å**	**1.477 Å**	**1.451 Å**
MP2/6-31G*	**N–N**	**1.815 Å**	**1.733 Å**	**1.688 Å**	**1.691 Å**	**1.659 Å**
B3LYP/6-31G*	**N–N**	**1.739 Å**	**1.733 Å**	**1.638 Å**	**1.634 Å**	**1.607 Å**

N$\rightarrow$O bond length is too short by 0.027 Å.

It is noteworthy that the AM1 N–N bond length (1.623 Å, bond order 0.553) is more reliable than the PM3 value (1.730 Å), although the other bond lengths moderately deviate from the observed values. However, the AM1 optimization does not reproduce the N–N bond length of all types, which is deduced from the model calculation of the five- and six-membered cyclic 1,2-dioxides (**A** and **B** in Fig. 6). The N–N bond lengths for **A** and **B** were calculated to be 1.593 and 1.530 Å, respectively, though the net charges of the N$\rightarrow$O moieties are almost the same magnitude. Compound **4**[8] is a typical example in which the AM1 structure optimization is not applicable (see Fig. 10). The AM1 N–N bond length (1.535 Å) of **4** is significantly shorter than the observed value (1.617 Å).

These results suggest that semiempirical SCF methods are still weak in the calculation of sequential heteroatom–heteroatom bonds, although in the progress of the semiempirical SCF MO methods, major improvements have been found for N–N, N–O and O–O bonds.

The efficacy of the AM1 method for evaluation of the O–N–N–O atomic sequence is still unknown but we found that the X-ray N–N bond [1.493 Å (3)] of the cycloadduct of 3,5-bis(methoxycarbonyl)-4-oxopyrazole 1,2-dioxide and epoxynaphthalene is reproduced by the AM1 optimization within a standard deviation[1*b*)] (Fig. 7).

The overestimation of the N–N bond length by the PM3 method is considered to be due to the large polarization of the N$\rightarrow$O moiety (N: 0.732 and O: −0.455), whereas the AM1-calculated N and O charges are 0.238 and −0.261, respectively.

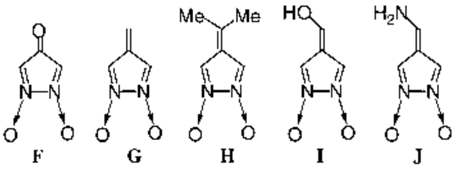

Chart 2

Based on the limits of the ability of semiempirical SCF calculation, the AM1 method is is recommended for calculation of 4-oxopyrazole 1,2-dioxide derivatives.

In general, bond elongations have been considered to arise from steric repulsion between the substituents attached to the bond in question. In the present case, the dipole–dipole repulsion of the parallelled highly-charged $N^+ \rightarrow O^-$ moieties is serious. The AM1 calculations of some donor- and acceptor-substituted 4H-pyrazole 1,2-dioxides (**A**, **C**—**E**) show that the N–N bond elongations due to the dipole–dipole repulsion would be *ca.* 1.59 Å, suggesting that the dipole–dipole repulsion is not the sole factor for the bond elongation.

Next, we inspected the N–N bond lengths of five model dioxides (**F**—**J**) having an exocyclic double bond at the 4-position.

Interestingly, the AM1 calculations of **F**—**J** indicate that substitution of the carbonyl moiety of 4-oxopyrazole 1,2-dioxide with more electron-rich ethylenes significantly shortens the N–N bond length [1.662 Å ($>$C=O)$\rightarrow$1.600 Å ($>$C=CH_2)$\rightarrow$1.551 Å ($>$C=$CHNH_2$)]. The *ab initio* calculations also showed a similar tendency regardless of the level of theory employed (Table 5). The elongation due to the substituent effect exceeds 0.11 Å in all the calculations.

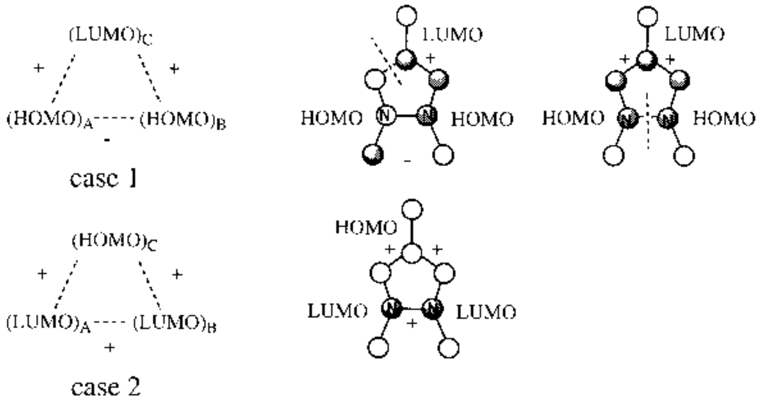

Fig. 8. Three–System Interaction

These results strongly suggest that the bond elongation is attributable to the electronic factor, *i.e.*, the aromaticity of the ring system.

The degree of cyclic electron delocalization can be qualitatively predicted in terms of the concept of cyclic conjugation based on the FMO theory (Fig. 8).[9)]

In three system interactions, there are two ways of dividing the systems by their roles. They are two donors and one acceptor (case 1) and two acceptors and one donor (case 2). In case 1, the orbital phase relation for stabilization has been found to be in phase (+) between the HOMO of donor A and the LUMO of acceptor C, in phase between the HOMO of donor B and the LUMO of acceptor C, and out of phase (−) between (HOMO)$_A$ and (HOMO)$_B$. In case 2, each relation should be in phase between (LUMO)$_A$ and (HOMO)$_C$, between (LUMO)$_B$ and (HOMO)$_C$, and between (LUMO)$_A$ and (LUMO)$_B$.

The molecules in question are divided into three parts, the exocyclic double bond and two nitrone moieties. Their donor/acceptor characters are estimated by considering the relative FMO energies of the corresponding unsubstituted compounds.

In the case of **F**, the nitrone moiety having a high-lying HOMO acts as a donor (D) and the carbonyl group acts as an acceptor (A). As shown in Fig. 8, the phase relation of **F** cannot satisfy the requirement of case one. On the other hand, **J** agrees with the requirement of case two, in which the aminoethylene acts as a donor and the nitrones act as an acceptor. These lead to the conclusion that **F** has an antiaromatic character whereas **J** has an aromatic character. The electron localization occurs in **F**, reflecting on the weakest N–N bond.

These considerations and conclusions are supported by the presence of a similar N–N elongation in furazano[3,4-*d*]pyridazine 5,6-dioxide (**4**) which can be predicted to be antiaromatic by the cyclic conjugation theory. The compound is composed of four functional groups, two endocyclic and two exocyclic double bonds. The donor–acceptor (D–A) arrangement of the four system is continuous but the orbital phase continuity is interrupted at the N–N bond. The X-ray N–N bond length of **4** is 1.617 Å, which is calculated to be 1.709 Å by the DFT calculation [B3PW91/6-31(2d)].

In summary, the first example of X-ray analysis of a 4-oxopyrazole 1,2-dioxide was presented. The extraordinary N–N bond elongation in 3,5-dimethyl-4-oxopyrazole 1,2-dioxide (**1**) is considered to arise from the dipole–dipole repulsion enhanced by the antiaromatic character of the ring system. The HF calculations underestimate N–N bond lengths. The reason is due to the lack of the configuration interactions on the calculation process. In contrast, the MP2 methods give too long bond lengths. These methods show a tendency to overestimate[10)] the effect of correlation which is improved when more advanced procedures like B3LYP or B3PW91 are applied. The observed structural features probably affect the cycloaddition behavior.

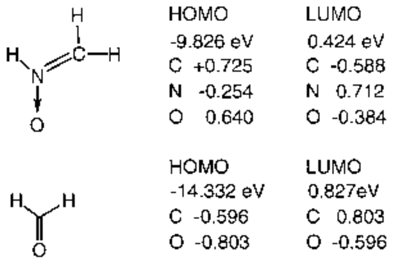

Fig. 9. FMO Levels and Coefficients of Parent Nitrone and Formaldehyde

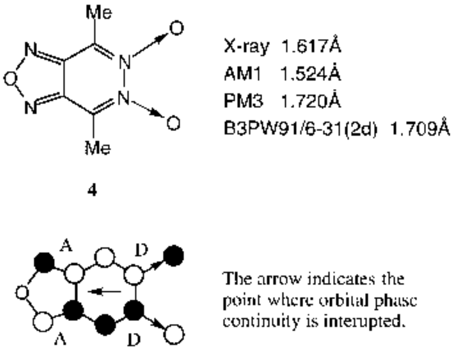

4

Fig. 10. X-Ray and Calculated N–N Bond Lengths of **4** and Its Cyclic Conjugation

Acknowledgement We thank Miss Aya Kamijikkoku for experimental assistance.

Reference and Notes

1) *a*) Eto M., Harano K., Yoshitake Y., Hisano T., *J. Heterocyclic Chem.*, **30**, 1557—1564 (1993); *b*) Eto M., Yoshitake Y., Harano K., Hisano T., *J. Chem. Soc.*, *Perkin Trans.* **2**, 1994, 1337—1345; *c*) Yoshitake Y., Eto M., Harano K., *Heterocycles*, **45**, 1873—1878 (1997); *d*) Yoshitake Y., Eto M., Harano K., *Tetrahedron Lett.*, **39**, 2761—2764 (1998).
2) *a*) Freeman J. P., Gannon J. J., Surbey D. L., *J. Org. Chem.*, **34**, 187—

194 (1969); *b*) Freeman J. P., Hoare M. L., *J. Org. Chem*., **36**, 19—23 (1971); *c*) Kotali A., Papageorgiou V. P., *Org. Prep. Proced. Int*., **23**, 611—616 (1991); *d*) Spyroudis S., Varvoglis A., *Chimika Chronika*, *New Series*, **11**, 173—179 (1982); *e*) Unterhalt B., *Tetrahedron Lett*., **15**, 1841—1845 (1968); *f*) *Idem*, *Arch. Pharm*. (*Weinheim*, *Ger*.), **300**, 822—827 (1967); *g*) Unterhalt B., Pindur U., *ibid*., **309**, 747—755 (1976).

3) Altomare A., Burla M. C., Camalli M., Cascarano M., Giacovazzo C., Guagliardi A., Polidori G., *J. Appl. Crystallogr*., **27**, 435 (1994).

4) Beurskens P. T., Admiraal G., Beurskens G., Bosman W. P., de Gelder R., Israel R., Smits J. M. M., (1994). The DIRDIF-94 program system, Technical Report of the Crystallography Laboratory, University of Nijmegen, The Netherlands.

5) Crystal Structure Analysis Package, Molecular Structure Corporation (1985, 1992).

6) a) Stewart J. J. P., *J. Am. Chem. Soc*., **107**, 3902—3909 (1985); *b*) *Idem*, *J. Comput. Chem*., **10**, 209—220 (1989), **10**, 221—264 (1989); *c*) AM1 and PM3 calculation are performed using MOPAC, Stewart J. J. P., *QCPE Bull*., **9**, 10 (1989).

7) Gaussian 94, Revision D.4, Frisch M. J., Trucks G. W., Schlegel H. B., Gill P. M. W., Johnson B. G., Robb M. A., Cheeseman J. R., Keith T., Petersson G. A., Montgomery J. A., Raghavachari K., Al-Laham M. A., Zakrzewski V. G., Ortiz J. V., Foresman J. B., Cioslowski J., Stefanov B. B., Nanayakkara A., Challacombe M., Peng C. Y., Ayala P. Y., Chen W., Wong M. W., Andres J. L., Replogle E. S., Gomperts R., Martin R. L., Fox D. J., Binkley J. S., Defrees D. J., Baker J., Stewart J. J. P., Head-Gordon M., Gonzalez C., Pople J. A., Gaussian, Inc., Pittsburgh PA, 1995.

8) Fruttero R., Ferrarotti B., Gasco A., Calestani G., Rizzoli C., *Liebigs Ann. Chem.*, **1998**, 1017—1023.

9) Inagaki S., Fujimoto H., Fukui K., *J. Am. Chem. Soc*., **98**, 4693—4701 (1976); Inagaki S., Hirabayashi Y., *ibid*., **99**, 7418—7423 (1977).

10) Sustmann R., Sicking W., Huisgen R., *J. Am. Chem. Soc*., **117**, 6979—9685 (1995).